

# Understanding cell fate decisions by identifying crucial system dynamics

Dirk Fey, David R. Croucher, Walter Kolch and Boris N. Kholodenko

## 1 Motivation

A hallmark of cancer is dysregulation of pivotal cell fate decisions leading to aberrant proliferation and reduced apoptosis. Healthy cell fate decisions depend on proper sensing of the cell's intra- and extracellular state in a processes called signal transduction. The usual scheme is that receptors sense signals by binding of an extracellular ligand, resulting in conformational changes that trigger the formation of multi-protein complexes and subsequent activation of GTPases and kinases. Hereby, one receptor usually activates several downstream pathways (Fig 1). A particular cell fate can usually not be attributed to the activity of a single protein in isolation, but rather depends on the context and temporal pattern of the activation and regulating feedback structures within the signalling network [21, 30, 19]. For example, treatment of Rat Pheochromocytoma (PC12) cells with epidermal growth factor (EGF) or nerve growth factor (NGF) activates the same signalling cascade (the RAF/MEK/ERK cascade) but has different effects on cell fate. EGF causes transient activation of extracellular regulated kinase (ERK) and proliferation due to negative feedback, whereas NGF causes sustained ERK activation and differentiation due to positive feedback [26, 37]. Because of this complexity, the function of cellular signalling often eludes a naive intuitive understanding, thus calling for the use of mathematical modelling and analysis [24, 16, 17, 23]. Here, we demonstrate

---

Dirk Fey

Systems Biology Ireland, University College Dublin, Ireland e-mail: dirk.fey@ucd.ie

David R. Croucher

Systems Biology Ireland, University College Dublin, Ireland e-mail: david.croucher@ucd.ie

Walter Kolch

Systems Biology Ireland, University College Dublin, Ireland e-mail: walter.kolch@ucd.ie

Boris N. Kholodenko

Systems Biology Ireland, University College Dublin, Ireland e-mail: boris.kholodenko@ucd.ie

how systems modelling and identification can be used to elucidate core processes underlying cellular decision making.

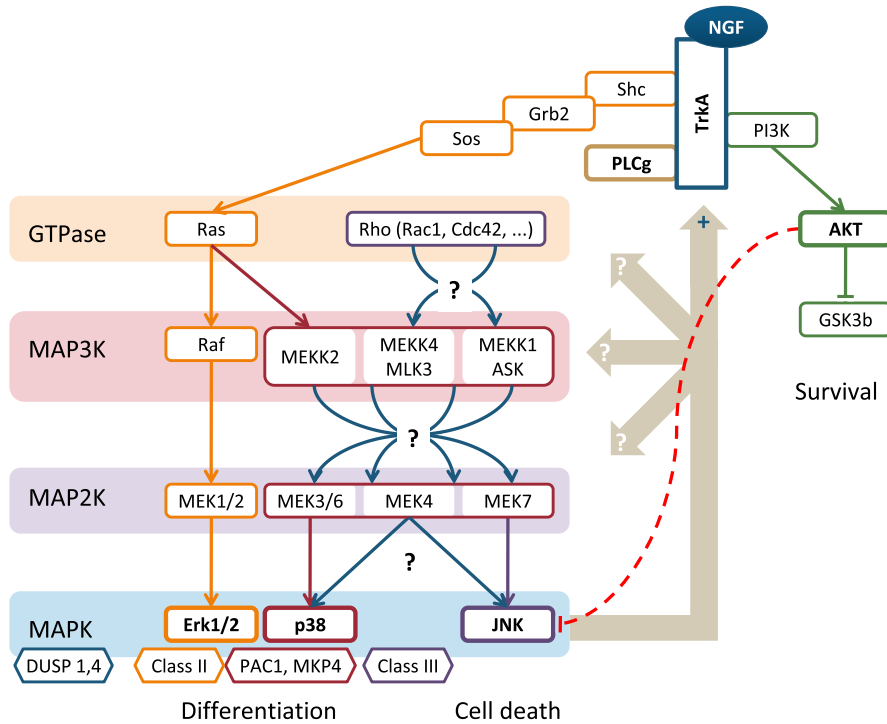


**Fig. 1** Signal transduction in a nutshell. After binding to its ligand a receptor (here TrkA) undergoes conformational changes, thus allowing the binding of several adaptor proteins, and triggers the activation of GTPases and kinases. Often the exact cascade of events is poorly understood and includes crosstalk and feedback.

## 2 Molecular biology and systems theory

Modelling biological systems on the intracellular level has been a research topic for over half a century. All started in 1943, when Erwin Schrödinger gave three talks in Dublin entitled *What is Life* [39, 40]. One of his central thoughts, and at that time a revolutionary idea, was that biological systems follow physical laws. In other words, biological systems can be described by mathematical models. For the control of membrane potential during neuronal excitation, this was achieved in 1952 by Hodgkin and Huxley, who explained and underlined their experimental data with a mathematical model, a key step in understanding how neurons function [14]. A

few years later, Denis Noble expanded this model to obtain the first mathematical model of the heart [31]. Nowadays, Hodgkin Huxley models and variants thereof are a vital part of computational neuroscience and widely used in research groups around the world. Part of Hodgkin and Huxley's success relied on the fact that they were able to estimate the model parameters from experimental data. In other areas of molecular biology, such as cell signalling and gene regulation, the identification of mathematical models has proven to be much more challenging.

The advances in biological experimental techniques of the last decades has led to a rapidly growing number of models [29, 27]. In signal transduction, the mitogen activated protein kinase (MAPK) downstream of the epidermal growth factor (EGF) was amongst the first systems to be modelled [15, 20]. From a modelling perspective, cell signalling systems are often composed of a number of similar modules or motifs, such as dimerisation processes or phosphorylation cycles. Biologically these modules are diversely implemented, i.e. composed of different molecular species. As a consequence, one particular module can exhibit very different behaviours, despite having the same interaction pattern. For example, the MAPK pathway consists of phosphorylation dephosphorylation cycles layered in three stages [21]. In nature, this scheme is implemented in several variations, involving different kinases such as ERK, JNK and p38. A model of a MAPK system can exhibit totally different behaviours such as homeostasis, near perfect adaptation and damped or sustained oscillations, depending on the values of the kinetic parameters [19]. This example illustrates the importance of choosing the correct parameters, especially if the model is to be used for predictions.

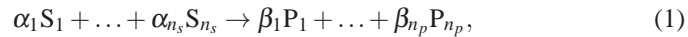
The main bottleneck in obtaining dynamic models of biological systems is the estimation of biological parameters, while structural information like stoichiometry are often known. Unknown parameters can be estimated from time-series data as is common practice in technical applications. Several peculiarities of biological systems hinder a straightforward application of most existing identification methodologies as typically used for technical systems. Biological systems usually have a large number of parameters, though often only a reduced set of experiments are possible, consisting of a few experimental steps and scarce time points. Furthermore, the noise level is usually significant.

Recent years have shown that the control system theoretical viewpoint and approaches are valuable tools for gaining a deeper understanding of biological systems [16, 44]. However, biological systems have particular properties, such as positivity and monotonicity, not often found in technical applications [41, 42]. This requires the design of novel methodologies particularly suited for biological systems. Concerning metabolic pathways, a prominent example is metabolic control analysis for sensitivity analysis developed in the 1970's [13, 8]. Metabolic control theory exploits the fact that enzyme concentrations vary on a much longer timescale than metabolite concentrations and metabolic systems spend most of their time resting in steady state, an assumption not sensible for signalling networks. Therefore, such unified theoretical treatments have not yet been established for signalling networks. This is partly due to the fact that signalling systems naturally deal with the temporal integration of ever changing extracellular conditions with the intracellular machin-

ery. As a consequence, the behaviour is often dominated by transient and nonlinear effects. In fact, the nonlinearity of signalling systems often generate the phenomena constituting particular biological functions. Examples are stable limit cycle oscillations in the case of circadian rhythms and cell cycles, or bistable switches in the case of cell fate decisions such as differentiation and apoptosis [28, 5]. From a theoretical perspective, the nonlinearity and behavioural complexity impedes the development of a (unifying) biological theory. As a consequence, the field is diversified with numerous theoretical works treating numerous specialised cases. This diversity is reflected in the recent release of books on the subject, such as *Systems Theory and Systems Biology* edited by Pablo Iglesias and Brian Ingalls [16] or *Systems Modelling in Cellular Biology* edited by Zoltan Szallasi, Jörg Stelling and Vipul Periwal [43] and the dedication of special issues on systems biology in the control community [1, 3]. We can however turn this argument around and exploit the particular form of biological nonlinearities [10, 12, 9, 2, 11, 7]. In this spirit, we present an identification methodology that is particularly tailored to biological systems and capable of estimating time-variant parameters.

## 2.1 Dynamic modelling

A common framework for the modelling of biochemical reaction networks involves sets of reactions of the following form



where  $S_i$  are substrates that are transformed into the products  $P_i$ . The factors  $\alpha_i$  and  $\beta_i$  are the stoichiometric coefficients of the reactants.

Neglecting spatial and stochastic effects, these reactions are often modelled with systems of ordinary differential equations:

$$\dot{c} = Nv(c, p), \quad (2)$$

where  $c \in \mathbb{R}_{\geq 0}^n$  is the vector of concentrations,  $p \in \mathbb{R}_{> 0}^{n_p}$  the parameter vector and  $v \in \mathbb{R}_{\geq 0}^n \times \mathbb{R}_{> 0}^{n_p} \mapsto \mathbb{R}_{\geq 0}^m$  the vector of the flows. The stoichiometric matrix  $N \in \mathbb{R}^{n \times m}$  depends on the coefficients  $\alpha_i$ ,  $\beta_i$  and, possibly on factors compensating different units or volumes. For a more detailed introduction, see for example [25, 18, 33].

There is a large variety of possible reaction models [?]. Here, we restrict the reaction models to the most common ones in signalling networks:

- mass action    The flow is proportional to each substrate:  $v = k \prod_{i \in I} c_i$  where  $I$  is a subset of  $1, \dots, n$  with possibly repeated entries;
- power law, S-Systems, generalised mass action    The flow is polynomial in the substrates:  $v = k \prod_{i \in [1, n]} c_i^{\alpha_i}$
- Michaelis-Menten or Monod    For low substrates the flow  $v$  depends linearly on the substrate  $s$  and saturates for large substrate concentrations at  $V_{\max}$ :

$v = V_{\max} \frac{s}{K_M + s}$ . At a substrate concentration of  $K_M$ , the flow is half the maximum rate.

**Hill** The flow is sublinear for low substrate and saturates for large substrate concentrations at  $V_{\max}$ :  $v = V_{\max} \frac{s^h}{K_M^h + s^h}$ . The exponent  $h$  is larger than one and at a substrate concentration of  $K_M$ , the flow is half the maximum rate.

In biochemical reaction modelling, the stoichiometry is usually known, as is the type of reaction kinetics, in contrary to the often quite uncertain parameters. Thus, the identification problem can be formulated as follows:

**Given:** The stoichiometric matrix  $N$  and the form of the function  $v(c, p)$  describing the reaction rates

**Unknown:** The kinetic parameters  $p$

Before we present the identification methodology, we discuss the effect of model approximations as models are by nature approximations of *real* systems.

## 2.2 Model approximations and time varying parameters

Dynamic models are mathematical descriptions of real processes. By nature, formalised descriptions are always approximate. The only model capturing all aspects of a real system is the system itself, or as Rosenblueth and Wiener expressed it "The best material model of a cat is another cat, or preferably the same cat" [36]. Nevertheless, mathematical models are helpful for understanding the behaviour of systems, especially if the underlying system is complex. The art of model building is therefore not to find the most accurate description, but the most helpful one. We have, therefore, to identify the core processes generating the considered behaviour. The process of identifying such a core model, awards us with an (basic) understanding of system that can be deepened by using mathematical analysis.

Complex models can be very accurate in the sense that simulating them replicates experimental data well. In contrast, simple models are usually associated with large quantitative discrepancies. From a theoretical perspective, matching a simplified model to a trajectory generated by a complex system, will result in time-varying parameters. We illustrate this fact using the system in Figure 2a. The input  $u$  regulates the formation and activity of several intermediate signalling molecules and complexes  $Z_1, \dots, Z_n$ . The output  $y$  is the intermediate molecule  $Z_n$ , which acts as enzyme for the phosphorylation of a downstream kinase  $X$ . Using Michaelis Menten kinetics, the rate of  $X$ -phosphorylation is

$$r_{\text{phos}} = k_{\text{phos}} z_n \frac{x}{K_1 + x}. \quad (3)$$

Assuming that the concentration of the intermediate molecules  $z_1, \dots, z_n$  are governed by a dynamic system, then  $z_n$  is a time varying variable, whose time course

depends not only on the initial conditions, but also the input  $u$ . We can find an approximate description of the rate  $r_{phos}$  in terms of the input by neglecting the dynamics of the intermediate variables. Assume for simplicity that the intermediate variables are described by a linear system of ordinary differential equations (Fig. 2b)

$$\dot{z} = Az + Bu, \quad (4)$$

$$y = Cz, \quad (5)$$

Formally, we obtain a quasi steady state approximation by setting  $\dot{z} = 0$  and solving for  $z$  (Fig. 2c)

$$z = A^{-1}Bu \Rightarrow y = CA^{-1}Bu. \quad (6)$$

Substituting (6) into (3) gives an approximate expression for the phosphorylation rate

$$r_{phos} \approx \underbrace{k_{phos} CA^{-1}Bu}_{=k_1} \frac{x}{K_1 + x}. \quad (7)$$

For constant inputs, (6) describes the steady state of the linear intermediate system. Thus, for a linear intermediate system in steady state, (3) is exact. In the dynamic case, the newly defined parameter  $k_1$  is time varying and approaches the value  $k_1 = CA^{-1}B$  for any input trajectory approaching steady state  $u(t) \xrightarrow{t \rightarrow \infty} u$ .

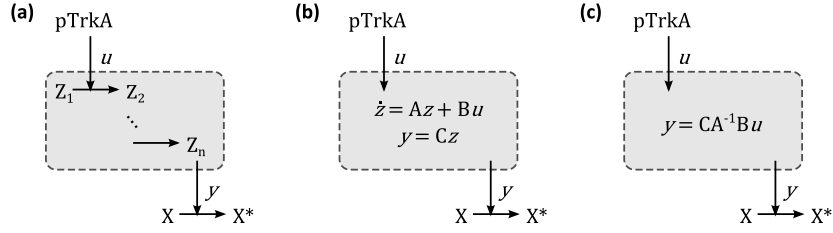


**Fig. 2** Conceptual scheme of TrkA signalling approximations. Phosphorylated TrkA (pTrkA) activates downstream kinases  $X$  via a system intermediates (grey box). (a) Most accurately, the intermediate system consists of a system of (unspecified) biochemical reactions. (b) Approximating the intermediate dynamics with a system of linear differential equations. (c) Quasi steady state approximation of the scheme in (b).

The above considerations motivate the following (oversimplified) model of kinase phosphorylation

$$\dot{x}^* = k_1 u \frac{x}{K_1 + x} - k_2 \frac{x^*}{K_2 + x^*}, \quad \text{where } x = 1 - x^*, \quad (8)$$

whereby we used the conserved moiety  $x_{tot} = x + x^*$  and normalised concentrations  $x_{tot} = 1$ . Because the model neglects the dynamics of the intermediate species, we

can imagine that trying to mimic experiments in simulations would perform rather poorly. However, this judgement is based on the assumption of constant parameters.

A consequence of neglecting the intermediate dynamics is that the parameter  $k_1$  is time-varying. Solving the system of linear differential equations (4) gives the time courses of the intermediates

$$z(t) = e^{At} \int_0^t e^{-A\tau} B u(\tau) d\tau,$$

where we assumed zero initial conditions  $z_i(0) = 0$ . By substituting into (3) and comparing to the simplified model (7) we see that the parameter  $k_1$  is a function of time

$$k_1(t) = C e^{At} \int_0^t e^{-A\tau} B u(\tau) d\tau \frac{k_{\text{phos}}}{u(t)}$$

Thus, trying to mimic experiments by simulating (8) would perform rather poorly and advanced identification techniques capable of estimating time-variant parameters are needed. Observers provide such a technique.

### 3 Parameter estimation with observers

The parameter estimation problem is closely related to the state estimation problem as both consider the estimation of unknown quantities. In loose terms, an observer is a mathematical system that estimates internal, non-measured states. Observer based approaches to parameter estimation require a certain system extension. Assuming that the parameters are constant, we can formally extend the state space with the parameters, i.e.

$$\begin{bmatrix} \dot{c} \\ \dot{p} \end{bmatrix} = \begin{bmatrix} f(c, p) \\ 0 \end{bmatrix}. \quad (9)$$

Note that the assumption  $\dot{p} = 0$  is a formal construct that enables us to formulate the problem mathematically. The same approach can be taken in order to estimate time varying parameters. Then the assumption  $\dot{p} = 0$  corresponds to a time scale separation of system dynamics and time varying parameters.

Given the above system, an observer can achieve a combined state and parameter estimation. However, designing observers for system (9) carries two difficulties: parameter dependency and nonlinearity. The parameter dependency triggers observability issues; for example, linearisations of (9) are generally not observable in steady state [7]. The nonlinearity of the problem means that the observer error depends on unknown states. For linear systems, the so called separation principle states that the dynamics of observer error only depend on the error itself and measured outputs [45]. Unfortunately, there is no separation principle for nonlinear systems. As a consequence, global convergence for all  $p \in \mathcal{R}$  can generally not be achieved [6, 4].

An alternative to the state space extension with  $\dot{p} = 0$  is the transformation into parameter free coordinates[9, 12, 2, 7]. The transformation exploits particular properties of biochemical reaction systems and facilitates the observer design. The entire identification procedure can be structured into three steps

1. Transformation of the system of ordinary differential equations into a parameter independent form;
2. Estimation of all states in the parameter free coordinates using an observer;
3. Back transformation to obtain the parameters.

In the following sections, we address each step in detail.

### 3.1 Transformation into parameter-free coordinates

This section presents the state space extension transforming the system into parameter free coordinates. The approach is first illustrated for a system with a single reaction, before the general extension scheme is presented.

*Example 1.* Let us consider the following system with  $k > 0$ ,  $K > 0$

$$\dot{c} = -v(c), \quad (10a)$$

$$v(c) = k \frac{c^2}{c + K}. \quad (10b)$$

Assuming that  $c$  and therefore  $v$  are positive, it is possible to derive the differential equation for the relative rate of change of the reaction rate, in essence taking the logarithm and time derivative of (10b). Before doing that, we introduce the new state

$$M = c + K$$

with the derivative

$$\dot{M} = \dot{c}.$$

Now, taking the logarithm and time derivative of (10b) gives

$$\begin{aligned} \frac{\dot{v}}{v} &= \frac{d}{dt} \log v = \frac{d}{dt} (\log k + 2 \log c - \log M) \\ &= 2 \frac{\dot{c}}{c} - \frac{\dot{M}}{M}. \end{aligned}$$

Substituting  $\dot{c} = -v$  yields the extended system

$$\begin{aligned}\dot{c} &= -v \\ \dot{M} &= -v \\ \dot{v} &= v \left( -2\frac{v}{c} + \frac{v}{M} \right)\end{aligned}$$

for which the right-hand-side is parameter free.

As the example illustrates, the states of the parameter free extended system consists of the concentrations  $c$ , the denominators of the reaction rates  $M$  and the reaction rates  $v$ .

In general, the approach considers reaction kinetic systems

$$\dot{c} = Nv(c, p, u), \quad (11a)$$

allowing for fluxes of the form:

$$v_i = k_i \prod_j \frac{c_j^{\alpha_{ij}} u^{\alpha_{u,ij}}}{M_{ij}} \quad \text{where} \quad M_{ij} = c_j^{\eta_{ij}} + K_{ij}, \quad (11b)$$

and where  $K_{ij} > 0$ ,  $\eta_{ij} \geq 0$  and  $\alpha_{ij}, \alpha_{u,ij} \geq 0$  denote known structural parameters and  $u \geq 0$  is a vector of inputs representing concentrations of unmodelled upstream components. If  $\eta_{ij} = 0$ , then the arbitrary parameter  $K_{ij}$  shall be equal to 1. The general formulation of (11b) contains mass action kinetics, generalised mass action kinetics, Michaelis-Menten- and Hill-kinetics as well as their products. For example, setting  $\eta_{ij} = 0$  leads to a mass action model, whereas setting  $\alpha_{ij} = \eta_{ij} = 1$  gives Michaelis-Menten kinetics.

For  $0 < \alpha_{ij} < 1$ , the flux  $v_i$  is not Lipschitz in  $c_j = 0$ . To ensure the existence and uniqueness of solutions, we assume that all concentrations are strictly positive.

**Assumption 1.** The parameters  $p$  and the concentrations  $c$  are strictly positive along trajectories of (9) and bounded, i.e.  $0 < \underline{\delta} \leq c_i(t, c_0) \leq \bar{\delta} < \infty$  holds for all species  $i$  and all initial conditions  $c_0$  for some positive constants  $\underline{\delta} < \bar{\delta}$ .

This condition is satisfied in many biological applications, in particular for models of metabolic pathways.

To simplify the presentation, define the following matrix-valued function  $M : \mathbb{R}_{\geq 0}^n \rightarrow \mathbb{R}^{m \times n}$

$$M_{ij} = K_{ij}^{\eta_{ij}} + c_j^{\eta_{ij}}. \quad (12)$$

Then the mapping

$$\Theta : \begin{bmatrix} c \\ p \end{bmatrix} \mapsto \begin{bmatrix} c \\ M(c, p) \\ v(c, p) \end{bmatrix} \quad (13)$$

is diffeomorph if Assumption 1 holds, defining a smooth and bijective state-space transformation of the original system (9) into an equivalent extended system that

is parameter free. This means, considering  $M_{ij}$  and  $v_i$  as additional states, complementing the natural states  $c_j$ , results in ordinary differential equations that do not depend on the parameters. The transformed system is

$$\dot{c} = Nv, \quad (14a)$$

$$\dot{M}_{ij} = \eta_{ij} c_j^{\eta_{ij}-1} e_j^T Nv, \quad (14b)$$

$$\dot{v} = \text{diag}(v) \left( \alpha (\text{diag}(c))^{-1} Nv + \alpha_u (\text{diag}(u))^{-1} \dot{u} - \tilde{m} \right), \quad (14c)$$

where

$$\tilde{m}_i = \sum_j \frac{\eta_{ij} c_j^{\eta_{ij}-1} e_j^T Nv}{M_{ij}}.$$

Summarising, any biochemical reaction model consisting of flows modelled as in (11b) can be transformed into a system that is free of parameters. In parameter free coordinates, the system is described using an extended state vector and depends only on structural properties of the original system.

The extended state is denoted by  $x \in \mathbb{R}_{>0}^{n_x}$

$$x = \begin{bmatrix} c \\ m \\ v \end{bmatrix}, \quad (15)$$

where  $m$  is the vector of all non-zero entries of

$$\text{vect}M = [M_{11} \cdots M_{m1} \ M_{12} \cdots M_{mm}]^T.$$

Assuming that the possibly time dependent inputs  $u_c = u_c(t)$  are differentiable, the dependence of the extended system on time derivatives of  $u_c$  does not pose a problem. We can define  $u^T = [u_v^T \ u_c^T \ \dot{u}_c^T]$  and write the system compactly as

$$\dot{x} = f(x, u) = \begin{bmatrix} Nv \\ f_M(c, v) \\ f_v(c, M, v, u) \end{bmatrix} \quad (16a)$$

*Remark 1.* Step and pulse inputs can be handled either using a differentiable approximation in the form of steep sigmoidal functions e.g.  $u_c = A_0(1 + \tanh(t - T_0))$  or by changing the initial condition accordingly and setting  $\dot{u}_c = 0$ .

To simplify the observer design, we introduce the assumption that the output is a subset of concentrations flows. This is the case in many biological applications.

**Assumption 2.** The output  $y(t) \in \mathbb{R}^{n_y}$  is a subset of concentrations  $c$  and flows  $v$ :

$$y = h \left( \begin{bmatrix} c \\ m \\ v \end{bmatrix} \right) = \begin{bmatrix} H_c & 0 & 0 \\ 0 & 0 & H_v \end{bmatrix} \begin{bmatrix} c \\ m \\ v \end{bmatrix}, \quad (16b)$$

where the matrices  $H_c$  and  $H_v$  are composed of columns of the identity matrices.

If some parameters values are already known, the proposed methodology can be adjusted in a straightforward way to not estimate them again. There are basically two cases. First, the parameter is a Hill or Michaelis-Menten constant  $K_{ij}$ . Then, there exists a state  $M_{ij}$ , which depends on  $K_{ij}$  and on some concentrations. This state can therefore be expressed as an algebraic equation of other states and does not require a differential equation. In the second case, the parameter is proportional to a flow, i.e.  $k_i$  in a flow  $v_j$ . This flow then also contains no unknown, only other states and thus its differential equation can be replaced by an algebraic equation. The reduced extended system is a differential algebraic system of index one. The algebraic equations can easily be eliminated, thus reducing the state space dimension by the number of known parameters.

### 3.2 Dissipative observer

Generally speaking an observer is an algorithm estimating internal states based on output measurements. Usually, observers consists of a copy of the system's equations and a correction term feeding back the estimation error, thus pushing the simulated trajectory towards the true trajectory [38]. In particular, the parameter free system (16a) facilitates the design of a dissipative observer [35, 9]. Let

$$A = \begin{bmatrix} 0 & 0 & N \\ 0 & 0 & 0 \end{bmatrix}, G = \begin{bmatrix} 0 \\ I \end{bmatrix} \text{ and } \Psi(x, u) = \begin{bmatrix} f_M(x, u) \\ f_v(x, u) \end{bmatrix},$$

then the parameter free system 16a writes as

$$\dot{x} = Ax + G\Psi(x, u), \quad (17a)$$

$$y = Cx, \quad (17b)$$

which is Lure's discretion into linear and nonlinear parts. A dissipative observer for (17) is

$$\dot{\xi} = A\xi + G\tilde{\Psi}(\xi + N \cdot (v - y), u) + L \cdot (v - y), \quad (18a)$$

$$v = C\xi, \quad (18b)$$

where the so called observer gain matrices  $N$  and  $L$  have to satisfy the linear matrix inequality (LMI)

$$\begin{bmatrix} -\frac{1}{\delta^2}I & I + NC & 0 \\ (I + NC)^T P(A + LC) + (A + LC)^T P + \varepsilon I & PG & \\ 0 & G^T P & -I \end{bmatrix} \preceq 0, \quad (19)$$

and the observer nonlinearity  $\tilde{\Psi}$  has to be constructed such that the mapping  $\Phi(z) : z \mapsto \tilde{\Psi}(x, u) - \Psi(x + z, u)$ , where  $\xi = x + z$ , satisfies the Lipschitz condition

$$\|\Phi(z, \sigma)\|_2 \leq \delta \|z\|_2.$$

A simple construction for the observer nonlinearity is

$$\tilde{\Psi}_i(x + z) = \begin{cases} \Psi_{\min} & \text{if } \Psi_i(x + z) > \Psi_{\min} \\ \Psi_i(x + z) & \text{if } \Psi_{\min} \leq \Psi_i(x + z) \leq \Psi_{\max} \\ \Psi_{\max} & \text{if } \Psi_i(x + z) < \Psi_{\max} \end{cases},$$

where  $\Psi_{\min}$  and  $\Psi_{\max}$  respectively are lower and upper bounds on the elements of  $\Psi$  on the true trajectory  $x(t, x_0)$ , i.e. it holds that

$$\Psi_{\min} \leq \Psi(x(t, x_0)) \leq \Psi_{\max}.$$

### 3.3 Obtaining the parameter estimate

The last step is the back transformation into original coordinates, which gives the actual parameter estimate. Inversion of (13) yields an explicit expression. In particular, using (12), the parameters  $K_{ij}(t)$  can be estimated via

$$\hat{K}_{ij}(t) = \begin{cases} (\hat{M}_{ij}(t) - \hat{c}_j(t))^{1/\eta_{ij}} & \text{for } \eta_{ij} > 0, \\ 1 & \text{for } \eta_{ij} = 0. \end{cases} \quad (20a)$$

Finally, the estimation of the parameters  $k_i(t)$  is possible using (11b)

$$\hat{k}_i(t) = \hat{v}_i(t) \prod_j^{n_c} \frac{\hat{M}_{ij}(t)}{\hat{c}_j(t)^{\alpha_{ij}} u(t)^{\alpha_{u,ij}}}. \quad (20b)$$

Because the observer has to be initialised with an unknown initial condition, the parameter estimate is time dependent. It converges to the true, constant values if and only if the observer converges.

### 3.4 Solutions to issues arising in praxis

Existence of the observer (18) depends on the feasibility of the LMI (19). A necessary condition is that the pair  $(A, C)$  is observable [9]. Unfortunately, this condition requires that Hill variables and linearly dependent rates are measured, which can not be achieved in praxis. We can overcome this problem by assuming that some parameters are known and create fake measurements as follows

- If the  $K_{ij}$  are known and  $y_c(t) = c(t)$  is measured, we can create fake measurements of the Hill variables:

$$y_M(t) = M(c(t), p) = M(y_c(t), K),$$

where  $K = [\dots, K_{ij}, \dots]$  is known and the elements of  $M$  are given by

$$M_{ij} = c_j(t)^{\eta_{ij}} + K_{ij}^{\eta_{ij}} = y_{c,j}(t)^{\eta_{ij}} + K_{ij}^{\eta_{ij}}$$

- If for some  $i$  the  $k_i$  and  $K_{ij}$  are known and  $y_c(t) = c(t)$ , is measured, we can create fake measurements of the fluxes :

$$y_{v,i}(t) = v_i(c(t), p) = v_i(y_c(t), p_i),$$

where the vector  $p_i$  contains the known parameters  $p_i = [k_i, K_{i1}, K_{i2}, \dots]$ .

The following section demonstrates the power of the observer based approach in praxis.

## 4 Application to TrkA induced MAPK signalling

Signalling via the neurotrophin receptor TrkA is known to be involved in embryonal formation of the neural system through a developmentally controlled expression pattern facilitating a process of neurotrophism and terminal differentiation [34]. Interestingly TrkA is also expressed in neural-derived tumours such as neuroblastoma, an embryonal tumour which arises in the para-vertebral sympathetic ganglion and adrenal medulla. Neuroblastoma tumours expressing high levels of TrkA have an exceptionally good prognosis, with the tumour frequently undergoing spontaneous regression, however the mechanism behind this regression is poorly understood, but should be linked to the regulatory machinery downstream of TrkA. Activation of the TrkA receptor by stimulation with the nerve growth factor (NGF) activates several signalling pathways and downstream kinases involved in cell fate decisions. The ability of TrkA to induce either proliferation, apoptosis or differentiation in vitro depending on the cell type and experimental design suggests a remarkable plasticity within the TrkA signalling network. In order to decipher the regulatory machinery

behind the multimodal response, we utilise a combination of experimentation, dynamic modelling and systems identification.

We model the activation of measured TrkA downstream kinases as simple phosphorylation-dephosphorylation cycles of the form

$$\begin{bmatrix} \dot{x} \\ \dot{x}^* \end{bmatrix} = \begin{bmatrix} -1 & 1 \\ 1 & -1 \end{bmatrix} \begin{bmatrix} v_1 \\ v_2 \end{bmatrix} \quad \text{with} \quad \begin{aligned} v_1 &= k_1 u \frac{x}{K_1 + x}, \\ v_2 &= k_2 \frac{x^*}{K_2 + x^*}, \end{aligned} \quad (21)$$

where  $u$  denotes the level of phosphorylated TrkA receptor and  $x, x^*$  denote the level of unphosphorylated and phosphorylated kinase, respectively. For each kinase, the parameters  $k_1, k_2, K_1, K_2$  present unknown quantities that have to be identified from experimental data. In particular, we measured timecourses of phosphorylated TrkA, Akt, Erk, JNK, PLC $\gamma$  and p38 in a TrkA inducible neuroblastoma SY5Y cell line in response to treatment with 1, 10 and 100nM NGF using western blotting (Fig 4).

The application of the observer based approach requires that several practical issues are overcome. First, the observer requires time-continuous measurements, which we solve by curve fitting the sampled data. Using the Matlab curve fitting toolbox, we fit

$$u(t) = a((1 - \exp^{-t/b}) \exp(-t/c))^2 + d * t^n / (e^n + t^n),$$

to the phosphorylated TrkA data, since it captures the bimodal TrkA response nicely and smoothing splines to all other kinases (Fig 4). Second, the observer requires that some parameters are known in order to create fake measurements for Hill variables and linearly dependent rates (see Sec. 3.4). In our model, the two differential equations (21) are linearly dependent, which means that the observer can only estimate one time varying parameter; either  $k_1$  or  $k_2$ . In order to get estimates of all other parameters (and preliminary estimates of  $k_1$  or  $k_2$ ), we use a genetic algorithm (Fig. 3). These estimates are then used to create the necessary fake measurements for the observer. Simulating the observer with the output

$$y_i = [1 - x_i^*, x_i^*, K_{1i} + 1 - x_i^*, K_{2i} + x^*, v_{2i}(x^*)]^T$$

gives a time-varying estimate for  $k_1$ , whereas simulating with

$$y_i = [1 - x_i^*, x_i^*, K_{1i} + 1 - x_i^*, K_{2i} + x^*, v_{1i}(x^*)]^T$$

gives a time-varying estimate for  $k_2$ . Here,  $x_i^*$  is the measured phosphorylation level for each kinase  $i = \text{Akt, ERK, JNK, PLC}\gamma, \text{p38}$ , whereas all other entries are fake measurements.

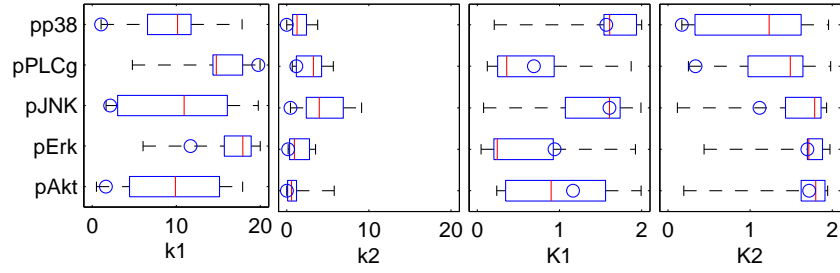


**Fig. 3** Parameter estimates of the genetic algorithm. Boxplots represent the distributions of final parameter estimates obtained from several runs of the genetic algorithm. The parameters were initialised from uniform distributions on the interval  $[0.1, 20]$  for  $k_1, k_2$  and  $[0.01, 2]$  for  $K_1, K_2$ . The red center mark indicates the medians, the edges of the box the 25% and 75% quartiles, the whiskers extend to the most extreme estimates and the circles indicate the best fit.

### Identification of time-variant parameters indicate a sensitive initial phase followed by desensitising adaptations

As expected, the parameter estimates of the observer are time varying. The simple model (21) neglects several intermediate signal transducers such as receptor adaptor proteins (SHC, GRB2, ...), GTPases (Ras, Rho, ...) and kinases (MEK, PI3K, ...) as well as pathway crosstalk and feedback structures. Thus, the parameters of the simple model are de facto functions of the neglected components. Because the neglected components change over time, the parameters of the simple model change over time. Indeed, at least two different phases can be distinguished, a highly sensitive initial phase, characterised by high values for the phosphorylation parameter  $k_1$  and low values for the dephosphorylation parameter  $k_1$ , followed by a delayed desensitisation phase, characterised by decreasing  $k_1$  estimates and increasing  $k_2$  estimates, suggesting the presence of desensitising feedback, for example in the form of phosphatase expression (Fig. 4).

### JNK estimate stands out, indicating that crucial dynamics are missing

Comparing the estimates for the 10nM and 100nM dose response, we notice remarkable differences for JNK. Generally, the 10nM and 100nM estimates are reasonably alike in the early phase (for  $t < 60\text{min}$ ) and follow similar trends in the late phase, at least for ERK, PLC $\gamma$ , and p38; however not for Akt and JNK. The Akt and JNK estimates exhibit opposing trends in the late phase. For example,  $k_1(t)$  decreases for the 10nM dose, but increases for the 100nM dose (Fig. 4). Comparing the relative differences of the 10nM and 100nM estimates for  $t = 240\text{min}$  reveals that the JNK difference is notably higher than that of the other kinases (Fig. 5). Together, these observations indicate that the simple model neglects some crucial dynamics affecting the JNK response and that model refinements are required.

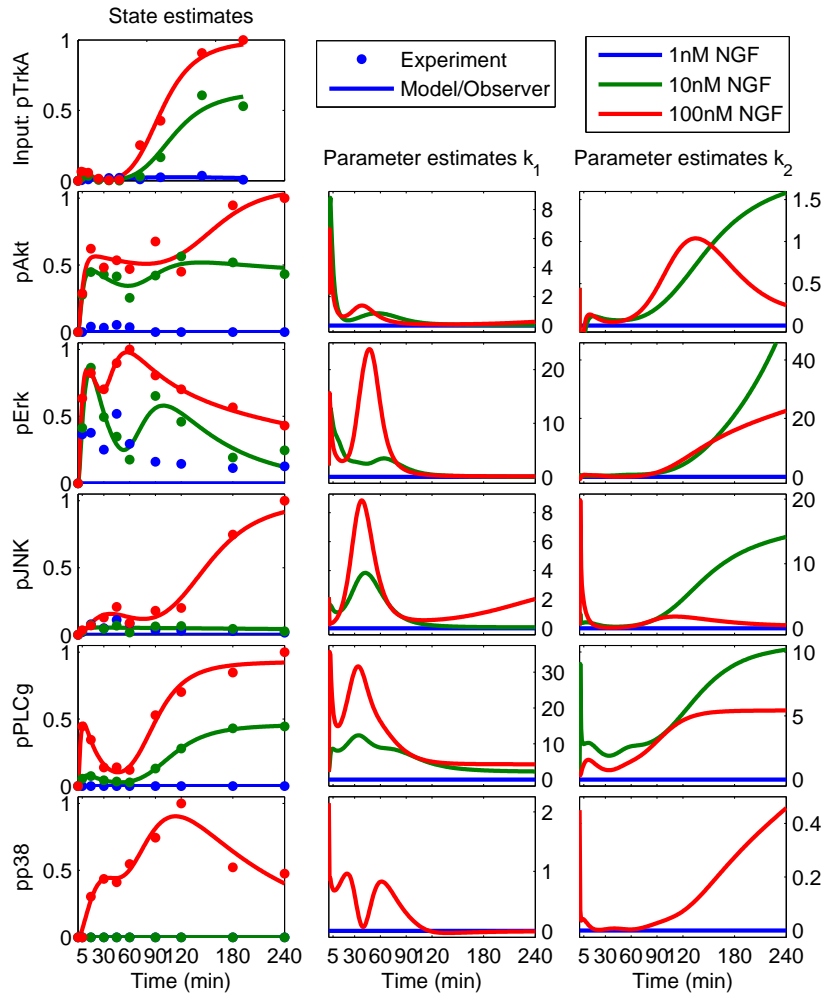


**Fig. 4** Time varying state and parameter estimates of the observer. The phosphorylation  $k_1$  and dephosphorylation  $k_2$  estimates were obtained in two different runs of the observer as explained in the main text. Because the 1nM (blue) dose did not produce detectable phosphorylation levels for most kinases, only the 10nM (green) and 100nM (red) responses were estimated. Further, no estimate was obtained for the p38 10nM response, because phosphorylation levels of p38 in response to 10nM NGF were not detectable in western blots. (a) Dots indicate measurements (quantification of western blots using imageJ), solid lines state estimates of the observer. (b) Estimates of  $k_1$ . (c) Estimates of  $k_2$ .

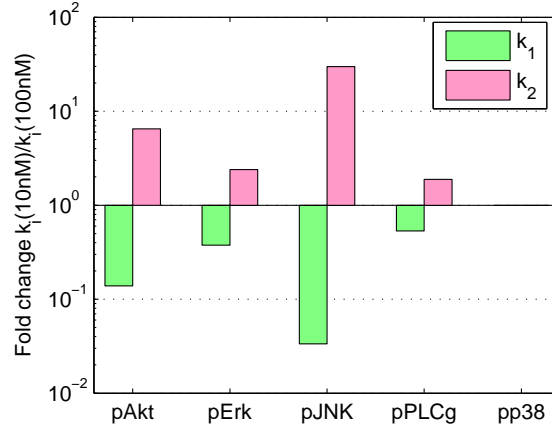


**Fig. 5** Fold change of parameter estimates for 10nM versus 100nM NGF at 240min. The JNK estimates markedly differ, showing a 30-fold change, (compared to < 6-fold for Erk and PLC $\gamma$ ). No estimate were obtained for p38, because phosphorylation levels of p38 for 10nM NGF were not detectable by western blotting.

### Refinement of the JNK model

Since our analysis hinted at JNK and Akt playing a special role in the systems response, we performed several follow up experiments. In particular, inhibition of JNK blocked the second phase of TrkA activation and NGF induced apoptosis (Fig. 6). In contrast, inhibition of AKT (using a PI3K inhibitor) significantly increased JNK phosphorylation and apoptosis (Fig. 6). The literature suggests that pAkt indirectly inhibits pJNK via phosphorylation and deactivation of JNK upstream kinases ASK1 and MKK4 [32, 22]. Taken together, these data suggest a model in which stimulation of TrkA phosphorylates and activates JNK, which in turn increases the levels of total and phosphorylated TrkA. Additionally, TrkA mediated activation of Akt inhibits phosphorylation of JNK (Fig 7). Neglecting the exact biochemical details, we can model the interaction scheme phenomenologically with two differential equations

$$\frac{d}{dt}P^* = k_P T^* \frac{P}{K_P + P} - k_{-P} \frac{P^*}{K_{-P} + P^*}, \quad (22a)$$

$$\frac{d}{dt}J^* = k_J T^* (1 - k_I P^*) \frac{J}{K_J + J} - k_{-J} \frac{J^*}{K_{-J} + J^*}, \quad (22b)$$

with  $P = 1 - P^*$ ,  $J = 1 - J^*$ , where  $P^*, J^* \in [0, 1]$  denote the level of active Akt and JNK, respectively. The term  $(1 - k_I P^*)$  models the inhibition of JNK phosphorylation by Akt, whereby the  $k_I \in [0, 1]$  denotes the inhibition strength with  $k_I = 0$  meaning no inhibition and  $k_I = 1$  complete inhibition. The level of TrkA activity is given by the algebraic equation

$$T^* = u(0.1 + J^*), \quad (22c)$$

where  $u$  denotes the strength of NGF stimulus and the term  $(0.1 + J^*) \in [0.1, 1.1]$  models the JNK mediated induction of TrkA with a basal TrkA level of 0.1 and maximal level of 1.1 (since  $J^* \in [0, 1]$ ). The advantage of this phenomenological formulation is that it facilitates the analysis of the systems core structure. (the two interlocked feedback loops) in a few parameters. The advantage of this formulation is that it describes the system's core structure in a few parameters, thus facilitating its identification and mathematical analysis. Indeed, the qualitative behaviour of the system is characterised by two parameters; the input strength  $u$  and the inhibition strength  $k_I$  and can be summarised in a three dimensional plot (Fig. 9), whereby the remaining parameters were chosen such that the simulated trajectories qualitatively mimic the recorded time courses (Fig. 8).

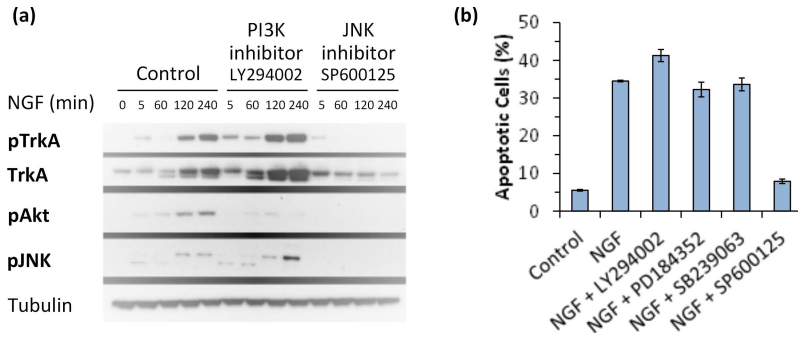


**Fig. 6** Results of inhibitor experiments. (a) Western blots of key components phosphorylated TrkA (pTrkA), total TrkA (TrkA), phosphorylated JNK (pJNK) and phosphorylated Akt (pAkt) at indicated time points after NGF treatment. JNK inhibition blocks the induction of total TrkA protein and the second phase of TrkA activation. PI3K inhibition increases TrkA and pTrkA levels and results in notably increased pJNK in the late phase. (b) Percentage of apoptotic cells. Apoptosis was assayed by propidium iodide staining and flow cytometry analysis. NGF induces high levels of apoptosis, which are blocked by inhibition of JNK. Inhibition of PI3K slightly increases the level of NGF induced apoptosis. LY294002 PI3K inhibitor, PD184352 MEK inhibitor, SB239062 p38 inhibitor, SP600125 JNK inhibitor.

**Fig. 7** Refined scheme of TrkA-JNK-Akt interactions. Solid lines represent (indirect) biochemical effects, with arrows indicating activation and bars indicating inhibition. The dotted circles indicate the two feedback loops present in the system.

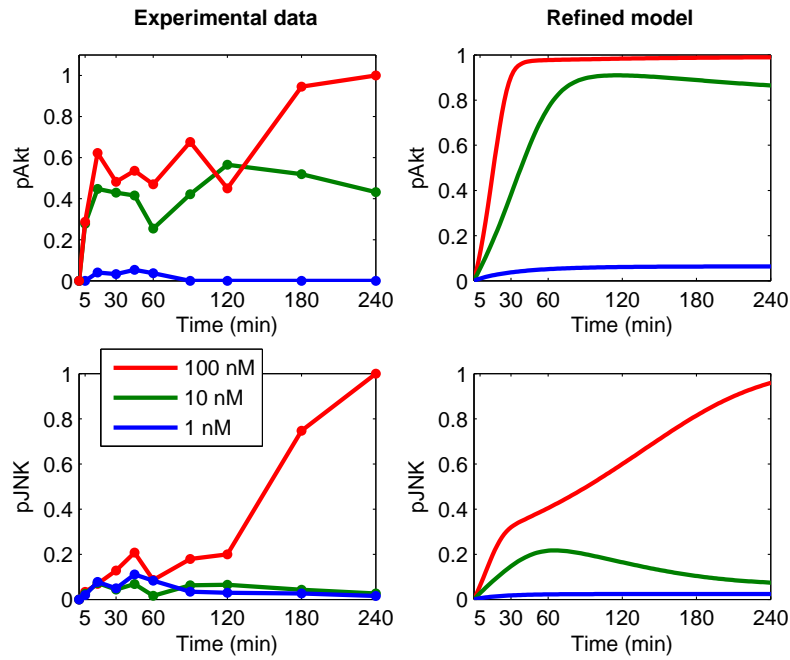
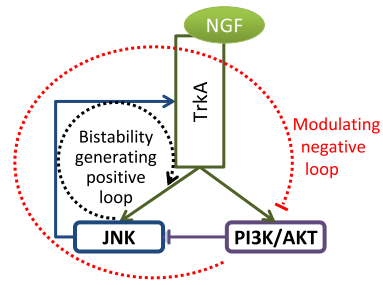


**Fig. 8** Qualitative fit of refined model. Left recorded timecourses, right trajectories of the JNK-Akt interaction model.

### Refined JNK model exhibits bistable behaviour

The refined TrkA-JNK-Akt interaction scheme contains two feedback loops generating complex system behaviour. For certain range of stimuli  $u$ , the positive feedback generates bistable behaviour, whereby the range at which bistability occurs depends on the strength of the negative feedback Fig. 9). Stronger Akt mediated inhibition of JNK (higher values of  $k_I$ ) shifts the bistable region to higher inputs. Thereby, the size of the JNK switch remains almost unaffected, whereas the size of the Akt switch decreases. For increasing  $k_I$  the Akt-off state approaches the Akt-on state until finally, high values of  $k_I$  cause the Akt switch to be so small that it can

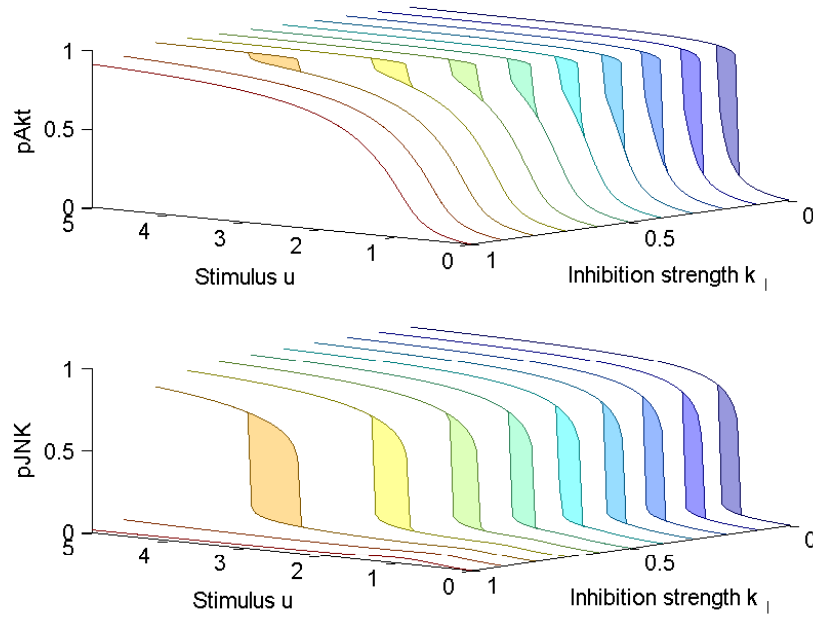


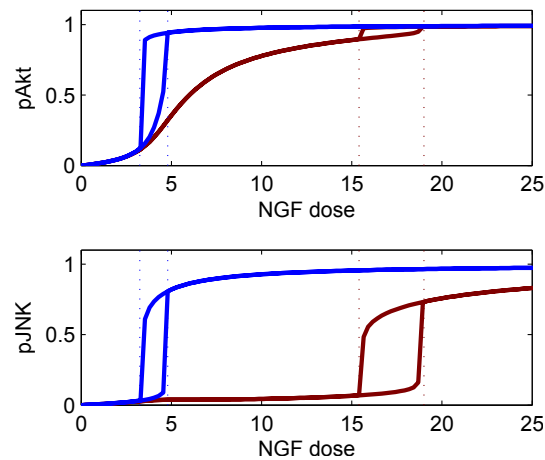
**Fig. 9** Complex behaviour of JNK-Akt interaction model summarised in bifurcation diagrams. The system exhibits bistability (patches). Increasing the parameter  $k_I$  (describing the strength of Akt mediated JNK inhibition) shift the range of inputs where bistability occurs to higher values and decreases the size of the Akt switch.

effectively be neglected (Fig. 10). Therewith, negative feedback provides a mechanism by which components normally affected by a bistable switch can effectively be decoupled.

### Concluding remark

Using the observer based approach, we identified the Akt-JNK interaction network as crucial component for TrkA induced apoptosis in a SY5Y neuroblastoma cell line. The time dependent variations of JNK and AKT associated parameters was markedly higher compared to other measured kinases, hinting at the neglect of crucial dynamics in a simple feedforward model and calling for model refinements. The refined JNK-Akt interactions model contains two feedback loops, and explains the switch to apoptosis with a bistable JNK response. For low stimuli the system is only transiently disturbed and quickly returns to the JNK off state, whereas high stimuli cause JNK to switch into its on state. The threshold at which the system switched depends on Akt mediated negative feedback. Unfortunately, the late phase activation of TrkA seems to be an artefact of the inducible cell line used. We are currently

**Fig. 10** Bifurcation diagram of the refined JNK-Akt model showing bistability. For increasing NGF stimuli, the JNK response remains almost unaffected (in the off state) until a certain threshold is reached at which JNK switches to the on state. For decreasing stimuli, the system switches back to the off state at a lower threshold, generating a hysteresis effect. For weak negative feedback (blue lines), Akt shows qualitatively behaviour similar to JNK, whereas for strong negative feedback (red) Akt exhibits a graded response. Blue and red lines correspond to  $k_I = 0$  and  $k_I = 0.8$ , respectively.



theinvestigating whether the obtained results are transferable to better neuroblastoma models in other cell lines. Nevertheless, the results demonstrate the power of the observer based approach and its applicability to real world data.

## 5 Conclusions

Dysregulation of cell signalling leading to tumourigenic cell fate decisions is a hallmark of cancer. Understanding this dysregulation requires the use of mathematical modelling and analysis. Since mathematical models are, by nature, approximations of the real system, the art of model building is therefore to find the correct level of abstraction. From a systems perspective, approximations result in time varying parameters, which are notoriously difficult to identify. Here, we presented a methodology capable of estimating time varying parameters. Importantly, time variant estimates indicate unmodelled dynamics and can be used to identify modelling errors. Strongly time-varying parameters point to modelling errors, and are the starting point for model refinements.

## References

1. Allgöwer, F., Doyle, F.: Introduction to the special issue on systems biology. *Automatica* **47**(6), 1095–1096 (2011). DOI 10.1016/j.automatica.2011.04.011. URL <http://www.sciencedirect.com/science/article/pii/S0005109811002317>. Special Issue on Sys-

- tems Biology
2. Bullinger, E., Fey, D., Farina, M., Findeisen, R.: Identifikation biochemischer Reaktionsnetzwerke: Ein beobachterbasierter Ansatz. *AT-Automatisierungstechnik* **56**(5), 269–279 (2008). DOI 10.1524/auto.2008.0703
  3. Chesi, G., Chen, L.: Call for papers: Special issue on systems biology. *International Journal of Robust and Nonlinear Control* **20**, 723–724 (2010)
  4. Dochain, D.: State and parameter estimation in chemical and biochemical processes: a tutorial. *Journal of Process Control* **13**(8), 801–818 (2003)
  5. Eissing, T., Waldherr, S., Allgöwer, F., Scheurich, P., Bullinger, E.: Steady state and (bi-) stability evaluation of simple protease signalling networks. *Biosystems* **90**(3), 591–601 (2007). DOI 10.1016/j.biosystems.2007.01.003. URL <http://dx.doi.org/10.1016/j.biosystems.2007.01.003>
  6. Farina, M., Bullinger, E., Findeisen, R., Bittanti, S.: An observer based strategy for parameter identification in systems biology. In: Proc. of the 2nd Conference on Foundations of Systems Biology in Engineering, Stuttgart, Germany, 521–526 (2007)
  7. Farina, M., Findeisen, R., Bullinger, E., Bittanti, S., Allgöwer, F., Wellstead, P.: Results towards identifiability properties of biochemical reaction networks. In: Proc. of the 45th IEEE Conference on Decision and Control, San Diego, USA, 2104–2109 (2006)
  8. Fell, D.: *Understanding the Control of Metabolism*. Portland Press, London (1997)
  9. Fey, D., Bullinger, E.: A dissipative approach to the identification of kinetic reaction networks. In: Proc. of the 15th IFAC Symposium on Systems Identification, Saint Malo, France, 1259–1264 (2009)
  10. Fey, D., Bullinger, E.: Limiting the parameter search space for dynamic models with rational kinetics using semi-definite programming. In: Proc. of the 15th Symposium on Computer Applications in Biotechnology, Leuven, Belgium, 150–155 (2010)
  11. Fey, D., Findeisen, R., Bullinger, E.: Parameter estimation in kinetic reaction models using nonlinear observers facilitated by model extensions. In: Proc. of the 17th IFAC World Congress, Seoul, Korea, 313–318 (2008)
  12. Fey, D., Findeisen, R., Bullinger, E.: Identification of biochemical reaction networks using a parameter-free coordinate system. In: Iglesias and Ingalls [16], 297–316
  13. Heinrich, R., Schuster, S.: *The Regulation of Cellular Systems*. Chapman and Hall, New York (1996)
  14. Hodgkin, A.L., Huxley, A.F.: A quantitative description of membrane current and its application to conduction and excitation in nerve. *J Physiol* **117**(4), 500–544 (1952)
  15. Huang, C.Y., Ferrell, J.E.: Ultrasensitivity in the mitogen-activated protein kinase cascade. *Proc Natl Acad Sci U S A* **93**(19), 10,078–10,083 (1996)
  16. Iglesias, P.A., Ingalls, B.P. (eds.): *Control Theory and Systems Biology*. MIT Press, Cambridge/MA (2009)
  17. Ireton, R., Montgomery, K., Bumgarner, R., Samudrala, R., McDermott, J. (eds.): *Computational Systems Biology, Methods in Molecular Biology*, vol. 541. Springer Verlag (2009)
  18. Keener, J., Sneyd, J.: *Mathematical Physiology, Interdisciplinary Applied Mathematics*, vol. 8, second edn. Springer-Verlag, New York (2001)
  19. Kholodenko, B.N.: Cell-signalling dynamics in time and space. *Nat Rev Mol Cell Biol* **7**(3), 165–176 (2006). DOI 10.1038/nrm1838. URL <http://dx.doi.org/10.1038/nrm1838>
  20. Kholodenko, B.N., Demin, O.V., Moehren, G., Hoek, J.B.: Quantification of short term signaling by the epidermal growth factor receptor. *J Biol Chem* **274**(42), 30,169–30,181 (1999)
  21. Kholodenko, B.N., Hancock, J.F., Kolch, W.: Signalling ballet in space and time. *Nat Rev Mol Cell Biol* **11**(6), 414–426 (2010). DOI 10.1038/nrm2901. URL <http://dx.doi.org/10.1038/nrm2901>
  22. Kim, A.H., Khursigara, G., Sun, X., Franke, T.F., Chao, M.V.: Akt phosphorylates and negatively regulates apoptosis signal-regulating kinase 1. *Mol Cell Biol* **21**(3), 893–901 (2001). DOI 10.1128/MCB.21.3.893-901.2001. URL <http://dx.doi.org/10.1128/MCB.21.3.893-901.2001>
  23. Kitano, H.: Systems biology: a brief overview. *Science* **295**(5560), 1662–1664 (2002). DOI 10.1126/science.1069492. URL <http://dx.doi.org/10.1126/science.1069492>

24. Kitano, H.: Grand challenges in systems physiology. *Front Physiol* **1**, 3 (2010). DOI 10.3389/fphys.2010.00003. URL <http://dx.doi.org/10.3389/fphys.2010.00003>
25. Klipp, E., Herwig, R., Kowald, A., Wierling, C., Lehrach, H.: *Systems Biology in Practice: Concepts, Implementation and Application*. Wiley-VCH, Weinheim (2005)
26. von Kriegsheim, A., Baiocchi, D., Birtwistle, M., Sumpton, D., Bienvenu, W., Morrice, N., Yamada, K., Lamond, A., Kalna, G., Orton, R., Gilbert, D., Kolch, W.: Cell fate decisions are specified by the dynamic erk interactome. *Nat Cell Biol* **11**(12), 1458–1464 (2009). DOI 10.1038/ncb1994. URL <http://dx.doi.org/10.1038/ncb1994>
27. Le Novère, N., Bornstein, B., Broicher, A., Courtot, M., Donizelli, M., Dharuri, H., Li, L., Sauro, H., Schilstra, M., Shapiro, B., Snoep, J., Hucka, M.: BioModels Database: A free, centralized database of curated, published, quantitative kinetic models of biochemical and cellular systems (2006). See also <http://www.ebi.ac.uk/biomodels/>, last visited 18 Jan 2012
28. Leloup, J.C., Goldbeter, A.: Modeling the circadian clock: from molecular mechanism to physiological disorders. *Bioessays* **30**(6), 590–600 (2008). DOI 10.1002/bies.20762. URL <http://dx.doi.org/10.1002/bies.20762>
29. Li, C., Donizelli, M., Rodriguez, N., Dharuri, H., Endler, L., Chelliah, V., Li, L., He, E., Henry, A., Stefan, M.I., Snoep, J.L., Hucka, M., Le Novère, N., Laibe, C.: BioModels Database: An enhanced, curated and annotated resource for published quantitative kinetic models. *BMC Syst Biol* **4**, 92 (2010). DOI 10.1186/1752-0509-4-92. URL <http://dx.doi.org/10.1186/1752-0509-4-92>. See also <http://www.ebi.ac.uk/biomodels/>, last visited 18 Jan 2012
30. Nakakuki, T., Birtwistle, M.R., Saeki, Y., Yumoto, N., Ide, K., Nagashima, T., Brusch, L., Ogunnaike, B.A., Okada-Hatakeyama, M., Kholodenko, B.N.: Ligand-specific c-fos expression emerges from the spatiotemporal control of erbb network dynamics. *Cell* **141**(5), 884–896 (2010). DOI 10.1016/j.cell.2010.03.054. URL <http://dx.doi.org/10.1016/j.cell.2010.03.054>
31. Noble, D.: Cardiac action and pacemaker potentials based on the Hodgkin-Huxley equations. *Nature* **188**, 495–497 (1960)
32. Park, H.S., Kim, M.S., Huh, S.H., Park, J., Chung, J., Kang, S.S., Choi, E.J.: Akt (protein kinase b) negatively regulates sek1 by means of protein phosphorylation. *J Biol Chem* **277**(4), 2573–2578 (2002). DOI 10.1074/jbc.M110299200. URL <http://dx.doi.org/10.1074/jbc.M110299200>
33. Reder, C.: Metabolic control theory: a structural approach. *J Theor Biol* **135**(2), 175–201 (1988)
34. Reichardt, L.F.: Neurotrophin-regulated signalling pathways. *Philos Trans R Soc Lond B Biol Sci* **361**(1473), 1545–1564 (2006). DOI 10.1098/rstb.2006.1894. URL <http://dx.doi.org/10.1098/rstb.2006.1894>
35. Rocha-Cózatl, E., Moreno, J.A.: Dissipative design of unknown input observers for systems with sector nonlinearities. *International Journal of Robust and Nonlinear Control* **21**, 1623–1644 (2011). DOI 10.1002/rnc.1656. URL <http://dx.doi.org/10.1002/rnc.1656>
36. Rosenblueth, A., Wiener, N.: The role of models in science. *Philosophy of Science* **12**, 316–321 (1945)
37. Santos, S.D.M., Verveer, P.J., Bastiaens, P.I.H.: Growth factor-induced mapk network topology shapes erk response determining pc-12 cell fate. *Nat Cell Biol* **9**(3), 324–330 (2007). DOI 10.1038/ncb1543. URL <http://dx.doi.org/10.1038/ncb1543>
38. Schaffner, J., Zeitz, M.: Variants of nonlinear normal form observer design. In: H. Nijmeijer, T. Fossen (eds.) *New Directions in nonlinear observer design, Lecture Notes in Control and Information Sciences*, vol. 244, 161–180. Springer Berlin / Heidelberg (1999). URL <http://dx.doi.org/10.1007/BFb0109926>. 10.1007/BFb0109926
39. Schrödinger, E.: *What is life* (1943). Dublin Institute for Advanced Studies, February 1943
40. Schrödinger, E.: *What is Life? The physical aspect of the living cell*. Cambridge University Press, Cambridge (1944)
41. Sontag, E.: Molecular systems biology and control. *Eur J Control* **11**(4–5), 396–435 (2005)
42. Sontag, E., Kiyatkin, A., Kholodenko, B.N.: Inferring dynamic architecture of cellular networks using time series of gene expression, protein and metabolite data. *Bioinformatics* **20**(12), 1877–1886 (2004). DOI 10.1093/bioinformatics/bth173. URL <http://dx.doi.org/10.1093/bioinformatics/bth173>

43. Szallasi, Z., Stelling, J., Periwal, V. (eds.): *Systems Modelling in Cellular Biology*. MIT Press, Cambridge, MA (2006)
44. Wellstead, P., Bullinger, E., Kalamatianos, D., Mason, O., Verwoerd, M.: The rôle of control and system theory in systems biology. *Annu Rev Control* **32**(1), 33 – 47 (2008). DOI DOI: 10.1016/j.arcontrol.2008.02.001. URL <http://www.sciencedirect.com/science/article/B6V0H-4SHFSTX-1/2/ad9687f1ea3e9d525c68c26d48b438ae>
45. Xia, X., Zeitz, M.: On nonlinear continuous observers. *International Journal of Control* **66**, 943–954 (1997)